Brownian dynamics simulation of charge transport in ion channels

2007 J. Phys.: Condens. Matter 19 215203

(http://iopscience.iop.org/0953-8984/19/21/215203)

IOP PUBLISHING JOURNAL OF PHYSICS: CONDENSED MATTER

J. Phys.: Condens. Matter **19** (2007) 215203 (16pp) doi:10.1088/0953-8984/19/21/215203

Brownian dynamics simulation of charge transport in ion channels

David Marreiro[1], **Marco Saraniti**[1] **and Shela Aboud**[2]

[1] ECE Department, Illinois Institute of Technology, Chicago, IL 60616, USA
[2] ECE Department, Worcester Polytechnic Institute, Worcester, MA 01609, USA

E-mail: marrdav@iit.edu, saraniti@iit.edu and saboud@gmail.com

Received 13 October 2006, in final form 13 December 2006
Published 1 May 2007
Online at stacks.iop.org/JPhysCM/19/215203

Abstract

In this work, we study the suitability of a P^3M force field scheme coupled with a Brownian dynamics simulation engine for the accurate modelling of charge transport in ion channels. The proposed simulation algorithm (Aboud *et al* 2004 *J. Comput. Electron.* **3** 117–33) is briefly discussed, and its validation for the electrodynamic description of aqueous solutions (Marreiro *et al* 2005 *J. Comput. Electron.* **4** 179–83; 2006 *J. Comput. Electron.* at press) is presented. The algorithm is applied to the simulation of ion channel systems where the influence of the dielectric representation and the diffusion coefficients are computed and compared to experimental (Van Der Straaten *et al* 2003 *J. Comput. Electron.* **2** 29–47) and simulated (Van Der Straaten *et al* 2003 *J. Comput. Electron.* **2** 29–47; Miedema *et al* 2004 *Biophys. J.* **87** 3137–47) data. The results show that while the bulk parameters do not correctly apply to the channel, the model can be refined by a careful choice of parameters in order to yield accurate charge transport properties while remaining extremely effective from the computational viewpoint.

(Some figures in this article are in colour only in the electronic version)

1. Introduction

The development of computational tools that are able to predict the ionic charge transport properties of biological ion channels based on their molecular structure is motivated by the availability of reliable experimental data on a large variety of channels and their recognition as highly valuable targets for pharmaceutical and engineering applications [6, 7].

Ion channels are challenging as far as simulation is concerned. The task of accurately predicting the electro-physiology of ion channels requires reliable modelling of each subsystem involved in the channel functions: the channel protein itself, the membrane within which the channel is inserted, and the electrolyte solution bathing the system. The simulation of each component presents its own challenges, such as the correct representation of electrostatic and

electrodynamic properties of the ion solutions, the polarization and short-range effects in the channel pores, and the modelling of the membrane and system boundaries.

The simulation is further complicated by the characteristic time and space scale of the ion channel system. The transport of charge in ion channels is a relatively slow process, with characteristic transit times of the order of nanoseconds or even microseconds, while the time resolution required to represent the ionic motion is in the femtosecond range. The spatial scale presents a similar challenge: the entire system has a nanometre size, while the particle trajectories have to be resolved within a fraction of an angstrom. A successful computer model will therefore need to describe the system very accurately in both time and space, while being able to do so for a relatively long simulation time in order to extract reliable and meaningful transport properties from the simulation data.

A variety of numerical approaches are currently used to simulate ion channel systems, from the very time-consuming molecular dynamics (MD) [8], which describes individually all the components of the system, to the inexpensive continuum models such as Poisson–Nernst–Planck (PNP) [9, 10] in which no particle is explicitly represented and both the ionic solution and the channel are modelled as continuous media. The purpose of this work is to demonstrate the capability of a cost-effective particle-based simulation tool to accurately and efficiently describe the charge transport properties of porins [11], a class of ion channels. The proposed approach is based on the coupling of a particle–particle–particle–mesh (P^3M) [12] force field with a Brownian dynamics (BD) [13, 14] engine. The P^3M force field has been applied successfully to the simulation of both semiconductor devices and ion channels [15, 16]. The use of Brownian dynamics makes this simulation tool less costly in terms of computation than an all-atom MD would be, because the solvent is represented implicitly and the total number of particles simulated is therefore greatly reduced. BD [17, 18] and MD [19] have already been applied to the analysis of ion channels. The novelty of the approach proposed here relies on the use of a real-space Poisson solver, enabling the simulation of a non-periodic system, which is not the case of MD simulations as in [19]. Furthermore, this method also accounts correctly for the effect of applied trans-membrane potentials by solving for the electric field resulting from the system charge distribution and applied boundary conditions.

In the following section, the working principles of the BD simulation approach are introduced, and a description of the system model is offered. References will be made to previous work [2, 3] conducted to validate the simulation model for electrolyte solutions and membranes in both equilibrium and dynamic settings. The subsequent section will describe the properties of the channels of interest to this work, and the simulation methodology. A section presenting the results will then be followed by discussion and conclusions.

2. Brownian dynamics simulation

The simulation tool proposed in this work is based on a self-consistent particle-based algorithm in which all the interactions within the system components are dependent on the spatial configuration of the components themselves, and on the externally applied boundary conditions. The forces exerted on the components are computed with a particle–particle–particle–mesh (P^3M) force field scheme, while the dynamics of the moving particles is updated within the BD formalism [1].

2.1. P^3M force field

Within the P^3M approach, the force exerted on each component of the system is computed through the sum of particle–particle (PP) and particle–mesh (PM) terms. This separation

is done for efficiency purposes. Indeed, a simple PP algorithm would be sufficient, for it computes the force on each particle as the direct sum of its pair interaction with every other particle in the system. However, its complexity scales with the square of the population N and it is prohibitively expensive in the case of ion channel systems where N is in the order of 10^5. In the P^3M framework, the PP summation is done over a small subset of the population containing the closest neighbours of the particle i being considered. The part of the force due to the interaction of particle i with the rest of the system components and the externally applied boundary conditions is then represented by the PM component which is computed on a discrete, real-space grid by an extremely fast iterative real-space Poisson solver [20]. The real-space solver can treat inhomogeneous, non-periodic systems, therefore allowing the direct application of an arbitrary trans-membrane potential in the simulation of ion channels. The details of the P^3M force field have been extensively discussed elsewhere [1]. The result of the P^3M force field computation is the force exerted on each particle by the entire system and the externally applied fields, which is then used in the Langevin equation to calculate the particle trajectory.

2.2. Langevin equation and integration

The proposed simulative approach achieves self-consistency by periodically freezing the particle dynamics after a small time interval called the free-flight timestep. The forces are then computed using the P^3M scheme while the particle velocities and positions are kept fixed. The dynamics is then resumed for the duration of the next free-flight timestep, which is of the order of 10–100 fs, and new positions and velocities are computed by solving the strict Langevin equation [14]:

$$m_i \frac{\mathrm{d}\vec{v}_i(t)}{\mathrm{d}t} = -\gamma_i^{\infty}\vec{v}_i(t) + \vec{F}_i(\vec{r}_i(t)) + \vec{B}_i(t), \tag{1}$$

where m_i is the mass of ion i, $\vec{v}_i(t)$ is its velocity at time t, and γ_i^{∞} its friction coefficient. The ion friction coefficient is derived from the diffusion coefficient using the Einstein relation (equation (2)) and represents the effects of water molecules on the ion dynamics. $\vec{F}_i$ denotes the force exerted by the rest of the system on the ion i, as obtained through the force-field computation. Finally, $\vec{B}_i$ is a random force representing the molecular bombardment of the water molecules on the ion i and is modelled as a Markovian random force.

Several integration schemes are available for the numerical solution of equation (1). These schemes limit the range of acceptable values for the free-flight timestep, which plays a crucial role in terms of computational performance and accuracy. The integration scheme is chosen to obtain the longest timestep possible while keeping the system energetically stable. Several schemes have been implemented, with varying complexities and merits in terms of accuracy and timestep requirements [3]. In this work, the second-order Verlet-like algorithm initially proposed by van Gunsteren and Berendsen [21] is used. The implementation of this integration scheme is described in [1]. It provides an optimal trade-off between cost and accuracy for the systems of interest here, as explained later in this section. The process of force computation and dynamics update is repeated as many times as needed to attain the desired amount of simulated time.

2.3. System model

In order to precisely define the characteristics of the model, each component of the system and its representation in the framework of the proposed simulation tool are described in this section. Within the BD formalism, the only moving particles are the ions of the electrolyte solution. Indeed, the effects of the solvent (water) on the electrostatics of the system are accounted for

implicitly by its (homogeneous) dielectric constant while its effects on the ionic dynamics are modelled through the friction coefficient and the random force in the Langevin equation. The friction coefficient is the only input parameter that governs the dynamics of the ions in the simulation. It is obtained from the experimental diffusion coefficients through the Einstein relation, which is applicable to BD models for molecular-sized particles [22]:

$$\gamma_i^{\infty} = \frac{k_B T}{D_i^{\infty}}, \tag{2}$$

where γ_i^{∞} is the friction coefficient for ion species i, D_i^{∞} is the experimental diffusion coefficient for this particular ionic species, k_B is Boltzmann's constant, and T is the system temperature. The superscript '$^{\infty}$' in equation (2) refers to the fact that the diffusion (and hence friction) coefficients used in the model are valid for bulk, infinitely dilute ionic solutions [23]. Whether using this diffusion coefficient is a valid choice within the P^3M framework is tested in this work and will be discussed in section 5.

We have chosen to represent the membrane as an impermeable dielectric barrier. This simple representation is likely to be a suitable choice in the case of porins, where the transport is not expected to be significantly affected by the external surface of the channel in contact with the membrane. On the other hand, the model chosen for the channel protein is an all-atom representation where the protein atoms are represented as fixed soft spheres with a Lennard-Jones [22] interaction potential, and the protein volume is given a specific relative dielectric value. Furthermore, the protein atoms bear electrostatic charges which are computed with the GROMACS [24] force field, using the standard protonation states assumed for a neutral pH. The porin molecule bears a total of −36 elementary charges in this case.

2.4. Simulation validation

A first step towards the successful simulation of highly complex systems like ion channels is to precisely define a set of benchmarks, and then compare them to simulation results for specific test systems. The accuracy, robustness, and validity of the simulation algorithm for a set of parameters can then be determined from these tests.

Preliminary work has been conducted [2] to validate the use of the extended primitive model for the electrolyte solutions of interest at concentrations in the biological range (up to 1 M). The bulk electrolyte solution was simulated at equilibrium and the radial distribution function (RDF) of the ions in solution was computed. The RDF was compared with results obtained with analytical computations for primitive model ionic solutions using the integral equations [25, 23] and the hypernetted chain (HNC) approximation [23, 26] as their closure relation [2]. In the same work, it was also shown that the use of the Verlet-like [21] integration scheme for the Langevin equation provided the best trade-off between accuracy and computational efficiency. The RDF and kinetic energy benchmarks for bulk electrolyte solutions at equilibrium have shown a correct and accurate representation of the thermodynamics and the structure of the solutions.

Further work was conducted [3] to validate an improved implementation of the Verlet-like integration scheme used in this work. The bulk solution was simulated with an externally applied voltage to compute conductivity and the results were compared to experimental conductivity measurements, showing the possibility of using free-flight timesteps in the 100 fs range while maintaining excellent accuracy for the dynamic transport properties of the ions. To validate the accurate representation of the structure of the electrolyte solution in the vicinity of a cell membrane, simulations were also performed with a dielectric membrane subjected to an externally applied trans-membrane bias. The resulting ion distribution in the vicinity of the membrane and the associated electrostatic potential were successfully compared [3] to the

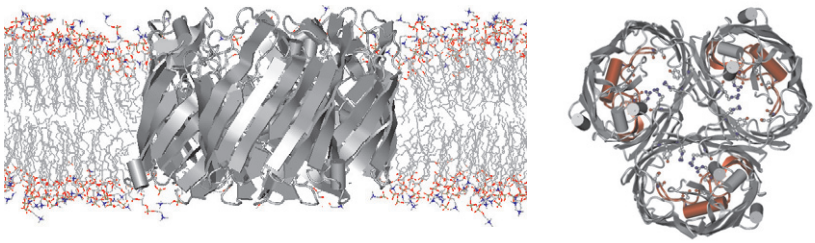

Figure 1. The OmpF porin channel from *E. Coli*, embedded in an explicit POPC membrane (left), and the corresponding top view of the OmpF alone (right). The picture is rendered with VMD [29] from the PDB database structure file 2omf.pdb [30, 11].

analytical results of the Gouy–Chapman double layer (DL) theory [22], therefore validating the use of free-flight timestep values up to 100 fs also for the simulation of inhomogeneous systems.

3. Charge transport simulation

3.1. OmpF channel

OmpF is found on the outer membrane of the bacterium *E. coli* [27]; it is a relatively large polypeptide made of three identical subunits containing 340 amino-acid residues each. OmpF is therefore a trimer, in which each monomer is a hollow cylindrical barrel structure formed by 16 anti-parallel β-strands [11, 28]. The molecular structure obtained from x-ray scattering experiments on protein crystals [11] shows chain loops forming a constriction region inside the pore. At the constriction, the pore lumen is reduced to a diameter of approximately 6 Å. Figure 1 shows side and top views of the trimer. The inner loops in the pore region are represented as shaded cylinders. It is important to note that the charged residue side chains in the small constriction region give rise to strong electric fields [4] that play a crucial role in the channel ionic transport properties and in its selectivity properties. The choice of the OmpF channel was motivated by the availability of experimental data as well as accurate crystal structures.

3.2. Simulation methodology

In section 2.3, the specifics of the representation of the electrolyte, membrane and protein were described. Throughout this work, the following assignments were made for the relative dielectric constants: the water dielectric constant was set to $\epsilon_{\text{water}} = 78$ throughout the system, while the dielectric membrane was chosen as having a relative dielectric of $\epsilon_{\text{membrane}} = 2$. The value of the dielectric constant of the protein is treated as a parameter of the simulation, as its effect on the simulation results is the object of this study. The values for the protein dielectric $\epsilon_{\text{protein}}$ were taken between 5 and 30. The dielectric constant is taken to be stepwise constant throughout the system grid (see section 2.1). The system grid uses a cell spacing of 1 nm in the bulk solution regions, and gradually reduces to a finer 0.4 nm grid spacing in the channel pore region. In some cases, the dielectric map was smoothed by the application of a simple moving average over the three-dimensional system grid. In those cases, the final dielectric constant in a cell was obtained as the arithmetic unweighted average of the preset cell dielectric value and that of its 26 neighbouring cells in space. For the cells adjoining the system

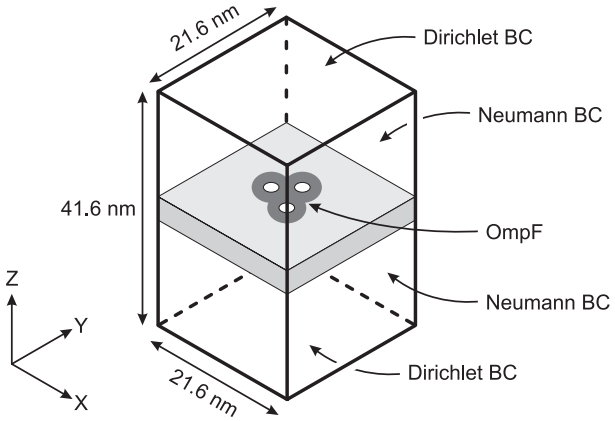

Figure 2. System model schematic showing geometry and boundary conditions.

boundaries, the average is taken on the dielectric values of the cells that are part of the system only. The simulations making use of a system grid obtained through this smoothing process will be referred to as smoothed dielectric simulations.

In this work, the dielectric constant of the pore lumen was always assumed to be equal to that of bulk water. It is important to note that some other studies have shown that different effective dielectrics may be used in the pore [31]. While this work has focused only on the effective protein dielectric representation, the methodology proposed here can be used with effective dielectrics in the pore as well, since the grid can be assigned an arbitrary, stepwise constant dielectric map and the real-space Poisson solver will account for it. We may therefore investigate the effect of such an effective dielectric representation of the pore lumen in later work, as it will clearly modulate the electric field strength in this critical region and impact the charge transport in the channel.

The system boundaries are non-periodic, which allows for the direct application of a trans-membrane electrostatic potential and avoids artefacts due to the application of periodic boundary conditions to extremely inhomogeneous systems. The system is enclosed in a computational box, the channel being positioned at the centre of the box, which is partitioned by the 4 nm thick dielectric membrane in the x–y plane (see figure 2). The transport therefore happens along the vertical z axis. The two opposite boundaries normal to the z axis are assigned Dirichlet boundary conditions [1], where the potential value is fixed in the first plane of cells adjacent to the system boundary. Furthermore, to account for the correct representation of the electrolyte and the effect of far electrodes, the concentration of ions and counter-ions is kept constant in these 'contact' cells through an appropriate injection/ejection algorithm [1]. To minimize the disruptive effect of the newly injected ions on the thermodynamic properties of the bath, they are injected with velocities following a Maxwellian distribution in the directions parallel to the contact cells, and a half-Maxwellian distribution in the direction normal to the contact cells. This injection process also ensures that the steady-state current flux established after a transient period does not deplete the system. The other four system boundaries are assigned Neumann boundary conditions, with the component of the electric field normal to the boundary set to zero and a specular reflection of the particles hitting the boundary.

The treatment of boundaries in BD simulations can significantly impact the charge transport in the channel, and several algorithms have been developed such as the grand canonical Monte Carlo [18] and a simple stochastic method [32]. In our case, the significant

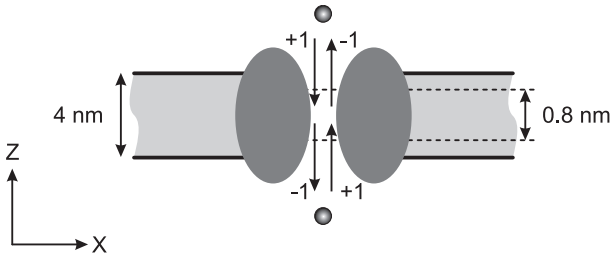

Figure 3. Pore openings model and current recording procedure.

buffer zone (more than 15 nm) set between the boundary and the channel ensures that the influence of the former is minimal. Indeed, we have also implemented other injection schemes including a displaced Maxwellian distribution for the injected ions, which have shown no effective influence on the ionic distributions and currents in the systems of interest. We have therefore retained the half-Maxwellian velocity distribution for the injected ions normal to the boundaries.

The time discretization of the system is determined by the free-flight timestep, and by the time interval between two consecutive solutions of Poisson's equation, the Poisson timestep, which is chosen to be 2 ps, much longer than the free-flight timestep. This is obviously done to save computation time, as the overall changes in the system charge distribution are much slower than the individual particle motions. Indeed, one estimator of the minimum frequency required for field updates is the plasma frequency of the ions, which is of the order of a few picoseconds in the case of biologically relevant aqueous solutions [1].

In order to compute the ionic currents in the channel and extract the related charge transport properties, the current flux of each ion species was recorded at the inner and outer openings of each pore in the channel. At the end of each free-flight timestep, particles crossing either boundary were recorded, and the total current flux was updated depending on the charge of the particle and the direction of the crossing. The resulting current flux curves for each particle are linearly increasing over time, and their slope, extracted with a least squares linear regression, yields the average current going through the pore opening. Finally, the total channel current is given by the average of the inner and outer currents in each of the three pores. Figure 3 shows how the current recording boundaries are set.

3.2.1. Validation of the methodology. In order to ensure that the integration scheme of the Langevin equation is used within its range of validity, a set of test simulations is run to choose an integration timestep that satisfies the accuracy requirements while providing the best computational efficiency. Figure 4 shows the evolution of the porin trimer conductance as a function of the integration free-flight timestep. The other simulation parameters are kept constant: a KCl bath concentration of 1.00 M, a protein region dielectric of $\epsilon_{\text{protein}} = 6$, an applied trans-membrane potential of 0.5 V, and reduced diffusion coefficients for the ions ($D_i = D_i'$; see table 1 for the numerical values used in this work). The trimer conductance is compared to experimental measurements from the literature [5], denoted with a dashed line in figure 4. It can be seen that for timestep values about 60 fs and below, the conductance remains relatively stable, with a numerical variability of around 1 nS. This numerical error is due to the very low number of particles crossing the pore (only of the order of 12 ns^{-1}). However, the average conductance obtained for simulations using timesteps smaller than 60 fs matches the experimental value when accounting for this numerical variability. The experimental value is

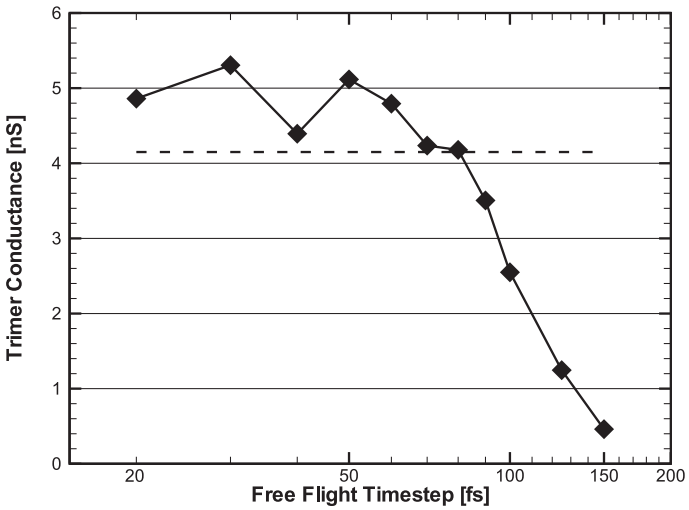

Figure 4. Porin trimer conductance as a function of the free-flight integration timestep, compared with an experimental measurement (dashed line) [5]. The bath concentration is 1.00 M and the applied trans-membrane potential is 0.5 V.

Table 1. Diffusion coefficient values used in this work. The superscript '∞' refers to infinite dilution or bulk values, while the reduced diffusion value D' is taken from [4].

	K^+	Cl^-
D^∞ ($m^2\ s^{-1}$)	1.960×10^{-9}	2.032×10^{-9}
D' ($m^2\ s^{-1}$)	0.630×10^{-9}	0.630×10^{-9}

known with a very high accuracy (5–10%, [33]), particularly at higher salt concentrations, as can be seen on the current traces as well [34, 4, 35, 36]. If the timestep used is greater than 60 fs, the conductance value gradually decreases. The less frequent integration of the Langevin equation and the consequent inaccuracies in the determination of the individual ion trajectories therefore reduce the simulation accuracy when the timestep is too large. The free-flight timestep value retained for all subsequent simulations was 50 fs, which was also shown [2, 3] to be well within the acceptable range of integration timesteps for the Verlet-like algorithm. This value of the timestep ensures that the structure of the electrolyte both in the bulk and in the vicinity of membranes is correctly represented [2, 3]. Choosing one of the largest acceptable integration timesteps obviously reduces the computational cost of the charge transport simulations.

4. Results

The system model is defined by several physical and numerical parameters. The difficulty presented by the timescale of charge transport phenomena in ion channels can be sidestepped by using higher concentrations and voltages unrealistic for such systems. Indeed, using larger voltages (of the order of 1 V) and concentrations in the molar range could provide statistically meaningful results with shorter simulation times. However, as a trans-membrane potential in excess of only 0.5 V effectively disrupts the bilayer structure [35], only voltages no greater than 0.5 V were used in this work, and between −200 and 200 mV in most cases. We are aware that the OmpF channel exhibits voltage gating and is closed most of the time when

the trans-membrane voltage is greater than 200 mV, as can be seen in current traces obtained with a ramped voltage [5]. However, the current–voltage curves measured experimentally [4] are almost linear, especially for high salt concentrations. Therefore, we are assuming that the calculated conductance of the open channel structure of OmpF under voltages between 200 and 500 mV is equal to that of the same channel under lower voltages.

In addition, the very high efficiency of the simulation and the choice of optimal parameters for the BD algorithm allowed us to restrain the concentrations used to a maximum of 1 M, allowing for the accumulation of statistically relevant results in runs of a few tenths of a nanosecond. This work was therefore restricted to the representation of realistic conditions for the ion channel system, and only the influence of the model parameters (dielectric and diffusion) which are not determined by the experimental setup (i.e., concentration and applied voltage) were tested.

4.1. The influence of the dielectric representation

Since the polarizability of the residues inside the channel pore is not explicitly represented in the model, the polarization effects are only accounted for by means of a dielectric constant. The validity of this choice is arguable; however, the OmpF constriction (7×11 Å^2 [37]) is wide enough to allow the permeation of small metabolites [27]. Therefore, the ions may remain at least partially hydrated as they move through the channel, in which case the implicit solvent and polarization representation is a reasonable approximation. This assertion will be discussed in light of the results presented in this work. The value of the protein dielectric constant affects how charged groups on the outside as well as the inside of the protein will influence the ions moving inside and around the pore, and will change the charge transport properties of the channel.

The system model uses the same dielectric value as water (78) inside the lumen of the pore; however, the first layer of cells that include the protein surface residues will have a different value. In the case of a smoothed dielectric map (see section 3.2), these cells will have a value between 40 and 50, which is the average of the water and protein dielectric constant. When smoothing is not used, those cells will be assigned the same dielectric value as the protein body, $\epsilon_{\text{protein}}$, which is chosen in the range of 5–20 since proteins are not a medium as polar as water. Figure 5 shows a cross section of the protein and membrane regions, in both smoothed and non-smoothed grid cases. It can be seen that the smoothing operation results in much higher dielectric for the protein surface regions, as well as less sharp interfaces, particularly in the pore region.

4.1.1. The protein/water interface in the pore lumen. In order to study the relative importance of the internal and surface dielectric representations of the protein, the following test was conducted. A first simulation was performed with a smoothed dielectric model, assigning $\epsilon_{\text{protein}} = 5$. The porin trimer total current was measured for a set of trans-membrane potentials varying between -200 and $+200$ mV, with a KCl concentration of 0.25 M in solution. A second simulation was performed with the same configuration, but a value of $\epsilon_{\text{protein}} = 20$ was assigned instead. Because of the smoothing, both configurations have very similar dielectric values on the protein surface, while the inner values are very different.

Figure 6 shows the two I–V curves obtained in these two cases. It can be seen that they are almost the same, which leads to the conclusion that the charge transport in the pore is mostly influenced by the dielectric representation of the surface of the protein (inside the pores), while the innermost part of the protein (and the associated dielectric constant) does not significantly affect the charge transport properties of the channel in this model. This is probably due to

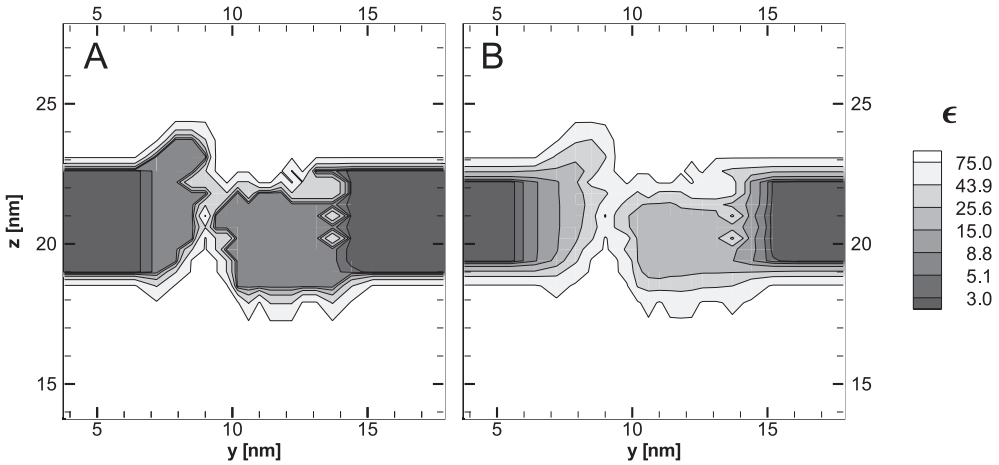

Figure 5. Dielectric map of the protein area as represented in the simulation. Section along y–z plane: (A) without smoothing, (B) with smoothing. $\epsilon_{\text{protein}}$ is set to 6 in both cases.

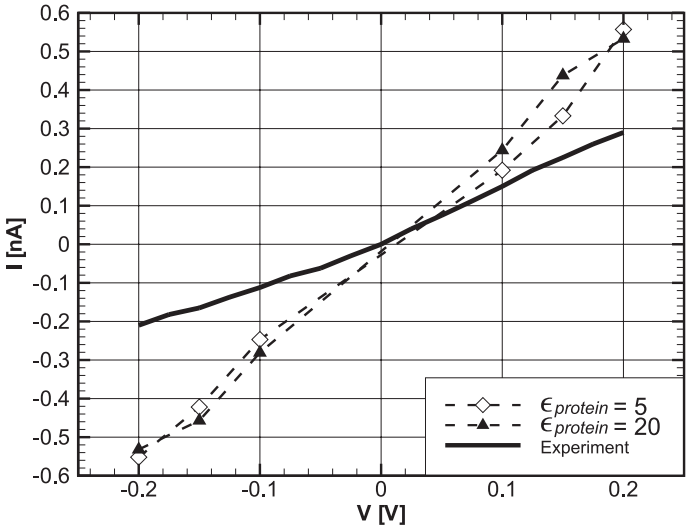

Figure 6. I–V curves obtained with a smoothed dielectric representation, with a 0.25 M KCl bath and applied trans-membrane potentials varying between −200 and +200 mV. Diamonds: $\epsilon_{\text{protein}} = 5$, triangles: $\epsilon_{\text{protein}} = 20$. Solid line: experimental measurement [4].

the fact that the inner charges inside the protein are effectively screened by the polarizable side chains on the loops inside the pores, preventing them from interacting strongly with the mobile ions in the pore, and therefore do not influence the charge transport in a measurable way. The calculated conductance under these conditions (KCl concentration of 0.25 M and voltage between −200 and 200 mV) is about 2.75 nS, while the experimental value is 1.25 nS [4]. The discrepancy is explained by the use of bulk diffusion coefficients in this set of computations, as will be shown in section 4.2.

4.1.2. The protein region dielectric constant. In order to assess the effect of the dielectric value chosen for the protein region, and especially for the surface within the pore constriction

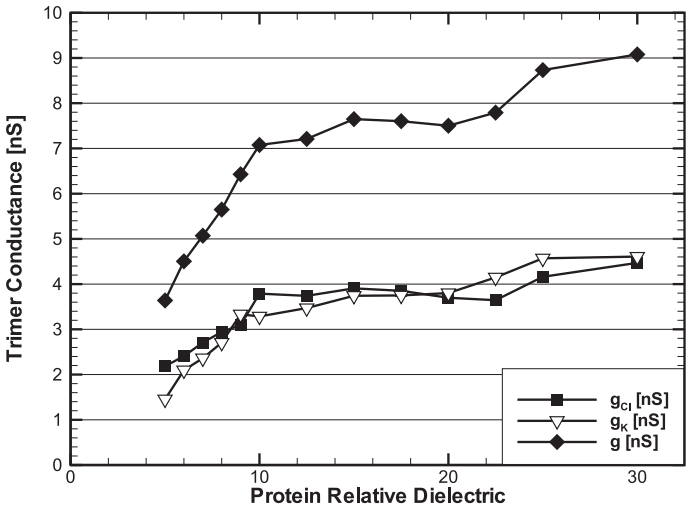

Figure 7. Channel conductances due to K^+, Cl^-, and trimer total conductance as a function of the protein relative dielectric. The KCl concentration is set to 0.25 M and the trans-membrane voltage is 500 mV.

region, tests are conducted in which the external conditions are maintained constant (KCl concentration of 0.25 M and trans-membrane voltage of 500 mV), while the dielectric constant of the protein region is varied between 5–30. The diffusion coefficient used in this case is the bulk diffusion D^{∞}. In this case, no smoothing of the dielectric map is used, so that the dielectric constant will be the same across the entire protein body and surface regions. Figure 7 shows the evolution of the trimer conductance due to K^+, Cl^- and the trimer total conductance as a function of $\epsilon_{\text{protein}}$. It can be seen that, for $\epsilon_{\text{protein}}$ values greater than about 10, the porin conductance is almost unchanged, while a significant drop in conductance is observed when $\epsilon_{\text{protein}}$ is taken below 10. As in figure 6, the computed conductances are well above the experimentally measured value of 1.25 nS, due to the use of bulk diffusion for the ions in the channel. However, the purpose of this set of computations is to show the strong dependence of the conductance on the protein dielectric chosen in the model.

To further study the importance of this choice, two sets of tests under different operating conditions are performed. Two series of computations, one using $\epsilon_{\text{protein}} = 6$ and the other using $\epsilon_{\text{protein}} = 20$ (no smoothing) were compared to experimental and PNP simulation results found in the literature [5, 4]. The KCl bath concentration was varied between 0.10 and 1.00 M and the diffusion coefficient used for the ions in this set of simulations is the reduced diffusion D' (see table 1). Each point is obtained by averaging the pore channel conductance computed under different trans-membrane potential values taken between −500–500 mV. Figure 8 shows the results of these computations. The error bars represent the standard deviation associated with this set of computations.

It can be seen that the set obtained for $\epsilon_{\text{protein}} = 6$ is relatively close to experimental measurements and PNP results, matching within the standard deviation in most cases. On the other hand, the results produced with $\epsilon_{\text{protein}} = 20$ show a consistently higher channel conductance (notably for concentrations above 0.5 M). This result is consistent with what was shown in figure 7, and can be explained as follows. It is known that the porin constriction region bears charged side-chains from aspartate, glutamate and arginine [28] which give rise to a strong transverse electric field inside the pore [4]. Figure 9 shows a map of the electrostatic

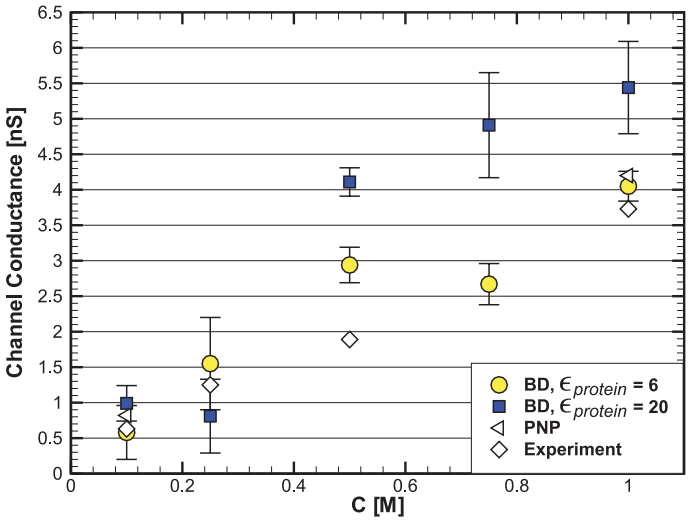

Figure 8. Trimer conductance as a function of bath KCl concentration. Circles: BD simulation with $\epsilon_{\text{protein}} = 6$, squares: BD simulation with $\epsilon_{\text{protein}} = 20$, triangles: PNP simulation [5], diamonds: experimental measurements [4].

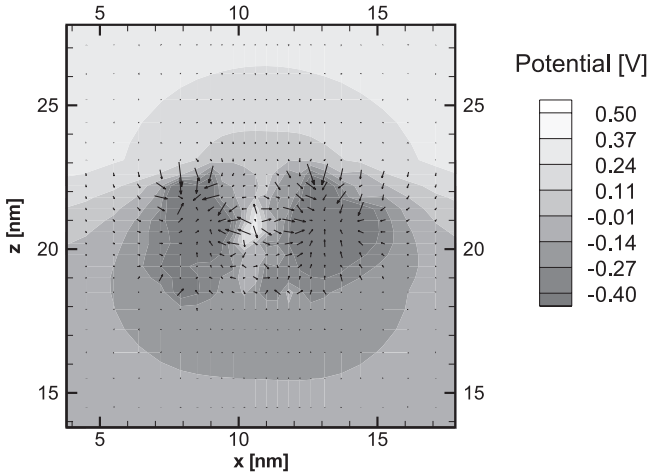

Figure 9. Electrostatic potential map of the porin under an applied field of 500 mV. Section along x–z plane. The arrows represent the electric field strength and direction.

potential along a cross section of one of the OmpF pores. The potential gradients show clearly negative average potentials inside the proteins, while the pore lumen is slightly positive. Furthermore, the electric field (represented by the arrows) is relatively stronger inside the pore and at the protein surfaces than inside the membrane or bath. It can be noted also that the map shows the transverse direction of the field in the pore constriction region.

This region thus forms a potential well for potassium ions and the assumed dielectric constant modulates the strength of the field and its effect on the moving ions inside the pore. A higher dielectric value reduces the field and facilitates the ionic motion, while a lower dielectric value increases the field. A stronger field increases the potential well and reduces the ionic

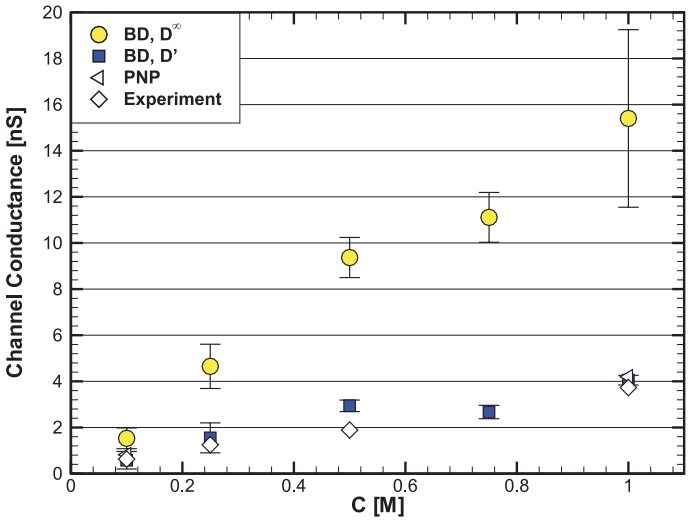

Figure 10. Trimer conductance as a function of bath KCl concentration. Circles: BD simulation with bulk diffusion D^{∞}, squares: BD simulation with reduced diffusion D', triangles: PNP simulation [5], diamonds: experimental measurements [4].

mobility in the pore. Comparison to experimental values shows that under the operating conditions used here (reduced diffusion D') the lower value of 6 for the protein dielectric provides a better representation.

4.2. The influence of the diffusion coefficients

The diffusion coefficient is a parameter of the simulation that has a direct influence on the charge transport properties of the channel. Unlike the dielectric constant, which influences the ion motion by modifying the electrostatic interaction between the charged groups on the protein surface and the ions, the diffusion coefficient modifies the dynamic behaviour of the ions in the framework defined by the Langevin equation. Indeed, a smaller diffusion coefficient means a higher friction coefficient (according to equation (2)), and thus a lower ionic mobility. Several diffusion coefficient schemes aimed at describing accurately the ion transport in the channel pores have been described in the literature [10, 4]. The diffusion coefficient can be set to specific 'local' values depending on the area of the pore that is considered (pore entrance on the intracellular side, pore constriction region, and pore exit on the extracellular side) such as in [10], or a single, system-wide diffusion coefficient value can be used as a fitting parameter to match experimental measurements [4].

In order to evaluate what diffusion coefficient provides the most appropriate description of the ion motion in the channel, two sets of values for the diffusion coefficients (D^{∞} and D') are used as inputs, and the channel conductance is computed and compared to experimental results. In both sets, the KCl bath concentration is varied between 0.10–1.00 M, while $\epsilon_{\text{protein}} = 6$. Again, each point is obtained by averaging the pore channel conductance computed with several trans-membrane potential values ranging between −500–500 mV, and the error bars represent the standard deviation associated with this set of computations. Figure 10 shows the results of these tests.

It can be seen that the bulk diffusion gives very high trimer conductances values, 3–4 times larger than experimental values under the same conditions. The use of the reduced diffusion

value (D', see table 1) produces results that are much closer to experiment. The reduced diffusion was proposed as a fit to experimental data for the PNP model [4]. It can be seen that the actual numerical value of the diffusion coefficients is about 3 times smaller than the bulk diffusion D^{∞}, which explains the lower conductance observed for the OmpF channel.

5. Discussion

The purpose of this work is to show the suitability of a P^3M force field scheme coupled with a Brownian dynamics simulation engine for the correct description of charge transport in ion channels. The OmpF channel is assumed large enough for the ions to be considered hydrated inside the channel. This implies the possibility of using bulk diffusion and dielectrics, and of describing the ions within the primitive model. The results obtained here with the P^3M BD simulations, as well as continuum models [4, 10], and their comparison with experimental data [4] (figures 8 and 10), show that using bulk dielectrics and diffusion inside the channel is not an accurate representation of the real system. However, it was also shown that this algorithm can be adjusted to provide very accurate results by carefully tuning the dielectric constants and diffusion coefficients in order to account correctly for the polarization in the pore region.

Much knowledge was gained in the process of developing and validating the algorithm. The details of the dielectric representation of the protein within the BD framework have been thoroughly studied and are now better understood. The meaning of the diffusion coefficient in bulk solution, and the possibility of extending it to the pore transport, have been studied as well. This knowledge, however, raises a new range of questions, which are already being investigated by experiments as well as other simulation approaches.

Indeed, the OmpF channel is represented as a static, all-atom structure in the proposed approach. Each atom is represented by a Lennard-Jones soft-core particle with a fixed partial charge obtained from the tabulated GROMACS [24] force-field. The values of these charges on the side-chains of the residues lining the pore is an absolutely critical component of the charge transport model, and it is therefore crucial to know the correct protonation states of the residues lining the pore as they undoubtedly have a strong influence on the charge transport process [38].

Furthermore, the actual protein structure is very mobile and charged side-chain groups change their conformation in the presence of an ion, altering its hydration state as it travels in the pore narrow region. It can be reasonably assumed that the strong fields present in this region affect the geometry of charged and polar groups by stretching and rotating bonds. This molecular polarization is not accurately represented by the fixed dielectric constant, if at all. The validity of using the crystal structure to represent the open state of the channel is, however, corroborated by the matching of experimental conductance results shown here, as well as the small deviation from the crystal structure observed in MD simulations [28].

Finally, the results have shown that the bulk diffusion parameters, while correctly modelling ionic transport in bulk solutions under a variety of conditions, are however erroneous in the case of transport inside a narrow channel. In fact, the bulk diffusion assumes a complete hydration shell around the ions as it represents the motion of ions in an infinitely diluted solution. The complete hydration shell is certainly not retained during transport, and the modality of the changes in this shell, the possible substitution of water by pore-lining residues, and the associated changes in the dynamics of charge transport are clearly not represented by the proposed approach.

Nevertheless, it is important to note that the model proposed here is extremely less costly in terms of computation than an all-atom MD would be. The use of empirical values for the dielectric constants and diffusion coefficients was proved successful in capturing the physics of charge transport inside the channel pores. The model can reasonably be applied to the study

of the charge transport properties of channels similar to OmpF, both wild-type and engineered, as well as analogous nanoscale structures such as decorated nanotubes, without the staggering cost of MD simulations.

6. Conclusion

A study of the suitability of a BD simulation using a P^3M force field scheme for the effective modelling of charge transport properties was performed by testing the relative importance and influence of critical model parameters such as the dielectric representation and the parameters governing the ion dynamics. A comparison was made between the results and published experimental and simulated data, and it was found that a careful choice of the model parameters yields an efficient and accurate model for charge transport in porin channels. Furthermore, a way to improve this model while maintaining its computational advantage was proposed.

Acknowledgments

We would like to thank Dr Larry H Scott and Dr Eric Jakobsson for their stimulating conversations and suggestions about this work.

References

[1] Aboud S, Marreiro D, Saraniti M and Eisenberg R 2004 A Poisson P^3M force field scheme for particle-based simulations of ionic liquids *J. Comput. Electron.* **3** 117–33
[2] Marreiro D, Aboud S, Saraniti M and Eisenberg R 2005 Error analysis of the Poisson P^3M force field scheme for particle-based simulations of biological systems *J. Comput. Electron.* **4** 179–83
[3] Marreiro D, Tang Y, Aboud S, Jakobsson E and Saraniti M 2006 Improving the efficiency of BD algorithms for biological systems simulations *J. Comput. Electron.* at press
[4] Van Der Straaten T A, Tang J M, Ravaioli U, Eisenberg R S and Aluru N R 2003 Simulating ion permeation through the OmpF porin ion channel using three-dimensional drift-diffusion theory *J. Comput. Electron.* **2** 29–47
[5] Miedema H, Meter-Arkema A, Wierenga J, Tang J, Eisenberg B, Nonner W, Hektor H, Gillespie D and Meijberg W 2004 Permeation properties of an engineered bacterial OmpF porin containing the EEEE-locus of Ca^{2+} channels *Biophys. J.* **87** 3137–47
[6] Hille B 2001 *Ionic Channels of Excitables Membranes* 3rd edn (Massachusetts: Sinauer)
[7] Ashcroft F M 2000 *Ion Channels and Disease* (San Diego, CA: Academic)
[8] Allen M P and Tildesley D J 1987 *Computer Simulation of Liquids* (Oxford: Clarendon)
[9] Barcilon V, Chen D-P, Eisenberg R S and Jerome J W 1997 Qualitative properties of steady-state Poisson–Nernst–Planck systems: mathematical study *SIAM J. Appl. Math.* **57** 631–48
[10] Chen D P, Tang J and Eisenberg B 2002 Structure–function study of porins *Technical Proc. 2002 Int. Conf. on Computational Nanoscience and Nanotechnology (NSTI Int. Conf. on Computational Nanoscience and Nanotechnology)* vol 2 (Cambridge, MA: NSTI) pp 64–7
[11] Cowan S W, Schirmer T, Rummel G, Steiert M, Ghosch R, Pauptit R A, Jansonius J N and Rosenbusch J P 1992 Crystal structures explain functional properties of two *E. Coli* porins *Nature* **358** 727–33
[12] Hockney R W and Eastwood J W 1988 *Computer Simulation Using Particles* (Bristol: Hilger)
[13] Ermak D L 1975 A computer simulation of charged particles in solution. I. Technique and equilibrium properties *J. Chem. Phys.* **62** 4189–96
[14] Turq P, Lantelme F and Friedman H L 1977 Brownian dynamics: its application to ionic solutions *J. Chem. Phys.* **66** 3039–44
[15] Wordelman C J and Ravaioli U 2000 Integration of a particle–particle–particle–mesh algorithm with the ensemble Monte Carlo method for the simulation of ultra-small semiconductor devices *IEEE Trans. Electron Devices* **47** 410–6
[16] Van Der Straaten T A, Kathawala G, Trellakis A, Eisenberg R S and Ravaioli U 2005 BioMOCA—a Boltzmann transport Monte Carlo model for ion channel simulation *Mol. Simul.* **31** 151–71

[17] Schirmer T and Phale P 1999 Brownian dynamics simulation of ion flow through porin channels *J. Mol. Biol.* **294** 1159–67
[18] Im W, Seefeld S and Roux B 2000 A grand canonical Monte Carlo-Brownian dynamics algorithm for simulating ion channels *Biophys. J.* **79** 788–801
[19] Im W and Roux B 2002 Ions and counterions in a biological channel: a molecular dynamics simulation of OmpF porin from Escherichia Coli in an explicit membrane with 1 M KCl aqueous salt solution *J. Mol. Biol.* **319** 1177–97
[20] Wigger S J, Saraniti M and Goodnick S M 1999 Three-dimensional multi-grid Poisson solver for modeling semiconductor devices *MSM99: Proc. 2nd Int. Conf. on Modeling and Simulation of Microsystems (Puerto Rico (PR), April 1999)* pp 415–8
[21] van Gunsteren W F and Berendsen H J C 1982 Algorithms for Brownian dynamics *Mol. Phys.* **45** 637–47
[22] Berry R S, Rice S A and Ross J 2000 *Physical Chemistry* 2nd edn (Oxford: Oxford University Press)
[23] Barthel J M G, Krienke H and Kunz W 1998 *Physical Chemistry of Electrolyte Solutions* (*Topics in Physical Chemistry* Number 5) (New York: Springer)
[24] Hermans J, Berendsen H J C, van Gunsteren W F and Postma J P M 1984 A consistent empirical potential for water-protein interactions *Biopolymers* **23** 1513–8
[25] Ornstein L S and Zernike F 1914 Accidental deviations of density and opalescence at the critical point in a single substance *Proc. Section of Sciences, K. Akad. Wet. te Amsterdam* **17** 793–806
[26] McQuarrie D A 2000 *Statistical Mechanics* (Sausalito, CA: University Science Books)
[27] Nikaido H and Vaara M 1985 Molecular basis of bacterial outer membrane permeability *Microbiol. Mol. Biol. Rev.* **49** 1–32
[28] Tieleman D P and Berendsen H J C 1998 A molecular dynamics study of the pores formed by Escherichia coli OmpF Porin in a fully hydrated palmitoyloleoylphosphatidylcholine bilayer *Biophys. J.* **74** 2786–801
[29] Humphrey W, Dalke A and Schulten K 1996 VMD-visual molecular dynamics *J. Mol. Graphics* **14** 33–8
[30] Karshikoff A, Spassov V, Cowan S W, Ladenstein R and Schirmer T 1994 Electrostatic properties of two porin channels from Escherichia Coli *J. Mol. Biol.* **240** 372–84
[31] Nonner W, Catacuzzeno L and Eisenberg B 2000 Binding and selectivity in L-type calcium channels: a mean spherical approximation *Biophys. J.* **79** 1976–92
[32] Corry B, Hoyles M, Allen T W, Walker M, Kuyucak S and Chung S-H 2002 Reservoir boundaries in Brownian dynamics simulations of ion channels *Biophys. J.* **82** 1975–84
[33] Saint N, Lou K-L, Widmer C, Luckey M, Schirmer T and Rosenbusch J P 1996 Structural and functional characterization of OmpF porin mutants selected for large pore size II *J. Biol. Chem.* **271** 20676–80
[34] Danelon C, Suenaga A, Winterhalter M and Yamato I 2003 Molecular origin of the cation selectivity in OmpF porin: single channel conductances vs free energy calculation *Biophys. Chem.* **104** 591–603
[35] Wilk S J, Goryll M, Laws G M, Goodnick S M and Thornton T J 2004 Teflon^{TM}-coated silicon apertures for supported lipid bilayer membranes *Appl. Phys. Lett.* **85** 3307–9
[36] Nestorovich E, Rostovtseva T and Bezrukov S 2003 Residue ionization and ion transport through OmpF channels *Biophys. J.* **85** 3718–29
[37] Alcaraz A, Nestorovich E M, Aguilella-Arzo M, Aguilella V M and Bezrukov S M 2004 Salting out the ionic selectivity of a wide channel: the asymmetry of OmpF *Biophys. J.* **87** 943–57
[38] Varma S, Chiu S-W and Jakobsson E 2006 The influence of amino acid protonation states on molecular dynamics simulations of the bacterial porin OmpF *Biophys. J.* **90** 112–23